JOURNAL OF VIROLOGY, Oct. 1998, p. 7754–7761 Vol. 72, No. 10
0022-538X/98/$04.00+0

Recombinant Measles Viruses with Mutations in the C, V, or F Gene Have Altered Growth Phenotypes In Vivo

ALEXANDRA VALSAMAKIS,[1] HENRIETTE SCHNEIDER,[2] PAUL G. AUWAERTER,[1] HIDETO KANESHIMA,[3] MARTIN A. BILLETER,[2] AND DIANE E. GRIFFIN[1]*

Molecular Microbiology and Immunology, Johns Hopkins School of Hygiene and Public Health, Baltimore, Maryland[1]; University of Zurich, Zurich, Switzerland[2]; and SyStemix, Palo Alto, California[3]

Received 29 April 1998/Accepted 11 June 1998

An understanding of the determinants of measles virus (MV) virulence has been hampered by the lack of an experimental model of infection. We have previously demonstrated that virulence phenotypes in human infections are faithfully reproduced by infection of human thymus/liver (thy/liv) implants engrafted into SCID mice, where the virus grows primarily in stromal cells but induces thymocyte apoptosis (P. G. Auwaerter et al., J. Virol. 70:3734–3740, 1996). To begin to elucidate the roles of the C protein, V protein, and the 5′ untranslated region of the F gene (F 5′UTR) in MV infection in vivo, the replication of strains bearing mutations of these genes was compared to that of the parent sequence-tagged Edmonston strain (EdTag). Growth curves show that mutants fall into two phenotypic classes. One class of mutants demonstrated kinetics of growth similar to that of EdTag, with decreased peak titers. The second class of mutants manifested peak titers similar to that of EdTag but had different replication kinetics. Abrogation of V expression led to delayed and markedly prolonged replication. Additionally, thymocyte survival was prolonged and implant architecture was preserved throughout the course of infection. In contrast, massive bystander thymocyte death occurred after infection with EdTag and all other mutants. A mutant which overexpressed V in Vero cells (V+) had the opposite phenotype of the A mutant not expressing V (V−). V+ grew more rapidly than EdTag with 100-fold-greater levels of virus production 3 days after infection. These results suggest that C, V, and the F 5′UTR are accessory factors required for efficient virus replication in vivo. In addition, thymocyte survival after V− infection suggests this protein may play multiple roles in pathogenesis of MV infection of thymus. Since these recombinant mutant viruses grew identically to the parent virus in Vero cells, the data show that thy/liv implants are an excellent model for investigating the determinants of MV virulence.

Measles virus (MV), a negative-strand RNA virus, was originally propagated in tissue culture by Enders and Peebles in 1954 (15). However, investigation of the molecular determinants of MV replication has been difficult, and the functions of a number of genes and control regions remain unknown. The rescue of infectious virus from a transfected cDNA clone has enabled the construction of the first recombinant mutant MVs (39) and has greatly facilitated such studies. The recombinant viruses examined to date grow identically to the parent virus in Vero cells (38, 39, 43), suggesting that the mutated genes and control regions are dispensable for MV replication in this cell line. The effects of these mutations on MV replication in vivo are not understood, in part because there is no small-animal model for measles.

We have previously used a human thymus xenograft, the SCID-hu thy/liv model, to characterize the replication and pathologic changes induced by vaccine and wild-type strains of MV known to differ in virulence (2). Thymus implants are created by coinoculation of human liver and thymus tissue under the renal capsule of a SCID mouse. Thymus cells give rise to the thymic microenvironment, and liver cells provide a source of hematopoietic precursors that populate the developing thymus (33). Three to four months postengraftment, a structurally and functionally normal thymus is formed. This model has been used to study the virulence of a number of other human viruses that lack small-animal models, including human immunodeficiency virus (HIV) (4, 22), cytomegalovirus (5, 30), and varicella-zoster virus (31, 32).

The SCID-hu thy/liv implant is a relevant model for examining the replication of MV strains in vivo since MV infects the thymus in natural disease. MV antigens and viral cytopathic effect have been found in thymus at autopsy following acute infection of humans (50) and at necropsy after experimental infection of primates (42). In vitro, primary cultures of human thymic stromal cells support MV growth (34). In addition, in vivo virulence phenotypes of MV are faithfully reproduced in thy/liv implants (2). Infection with the minimally passaged patient isolate Chicago-89 (Chi-1) strain results in high levels of virus replication in stromal cells and macrophages after 3 days of infection and massive thymocyte death. In contrast, growth of an attenuated Moraten vaccine strain is slow and causes little thymocyte death.

We have utilized the SCID-hu thy/liv system to investigate the role of the 5′ untranslated region of the F gene (F 5′UTR), the C protein, and the V protein in MV growth in vivo. Among the paramyxoviruses, only the F mRNAs of the morbilliviruses contain a long 460- to 580-nucleotide GC-rich region between the transcription start site and the methionine initiation codon. This region has been predicted to have extensive secondary structure (41). Experiments to define its function suggest that the F 5′UTR acts as a focusing factor, directing translation initiation from the second of four clustered AUGs (8). In addition, this region affects the efficiency of F translation. In DNA vaccination studies, the MV F 5′UTR is required for an effective anti-F antibody response in mice and therefore presumably for the expression of F (47). It is also required for

* Corresponding author. Mailing address: Dept. of Molecular Microbiology and Immunology, School of Hygiene and Public Health, Johns Hopkins University, 615 N. Wolfe St., Baltimore, MD 21205-2179. Phone: (410) 955-3459. Fax: (410) 955-0105. E-mail: dgriffin@welchlink.welch.jhu.edu.

rinderpest and canine distemper virus F-protein expression in immortalized cells using vaccinia virus-encoded T7 polymerase to express F mRNA (16). However, in other vaccinia virus-encoded T7 polymerase expression studies, partial deletion of the MV F 5′UTR results in increased F expression (10), and in rabbit reticulocyte lysates, the 5′UTR inhibits rinderpest and canine distemper virus F translation (16), suggesting that this region can also inhibit F translation.

The C protein is a small (~20-kDa), positively charged protein encoded within the P open reading frame (ORF) of the morbilliviruses and paramyxoviruses but not the rubulaviruses. MV expresses a single C protein from an alternative methionine downstream from the initiator for the P ORF (3). In Sendai virus (SeV) infection, a nested set of four C proteins, (C′, C, Y1, and Y2) with different translation initiation sites and common COOH termini are expressed (13, 18, 36). A number of studies have failed to identify C in purified virions, leading to its designation as a nonstructural protein. However, recent studies of SeV have found small amounts of C associated with the nucleocapsid in purified virions (51). In infected cells, C is found in the nucleus and the cytoplasm, where it colocalizes with nucleocapsids (3). The function of C is not clear. Studies with SeV suggest that C inhibits mRNA and antigenomic RNA synthesis (6, 45), perhaps through direct binding to L, the catalytic subunit of the viral polymerase (19). Whether C regulates MV polymerase in a similar manner is unknown.

The V protein is an ~40-kDa protein expressed from the P ORF of all paramyxoviruses except respiratory syncytial virus and parainfluenza virus types 1 and 3. In the paramyxovirus and morbillivirus families, V is a nonstructural protein synthesized as a result of polymerase slippage at a distinct site within the P ORF which leads to the pseudotemplated insertion of a single G residue (9, 12, 48). Thus, the amino terminus of V (231 amino acids in MV) is identical to that of P, acidic, and highly phosphorylated. The carboxy terminus is unique to the V protein (68 amino acids in MV), is highly conserved among the paramyxoviruses, and contains a cysteine-rich zinc finger domain which binds zinc (27). V is distributed diffusely in the nucleus and cytoplasm of infected cells and does not colocalize with nucleocapsids (12, 49). Analysis of SeV V function in transfected cells suggests that it inhibits genome replication by binding soluble nucleoprotein (20). In coimmunoprecipitation studies, MV V appears to bind a number of cellular proteins (28), but the relevance and role of these interactions are not yet clear.

The rubulaviruses encode V proteins which are structurally and functionally different from paramyxovirus and morbillivirus V proteins. Rubulavirus V proteins are structural proteins which associate with the nucleocapsid (35, 44). They are encoded directly in the viral genome (44, 46) and have shorter, basic amino termini. In simian virus 5, this region binds RNA and nucleoprotein (26, 37, 40). Like those of SeV and MV, the carboxy terminus of rubulavirus V is cysteine rich and binds zinc (35).

MV mutants which have a deletion of the F 5′UTR or mutations abrogating expression of C and V (C− and V− mutants) grow like the parent virus in Vero cells (38, 39, 43), and the growth of SeV V− is unaltered in a variety of cell lines (14). To determine whether these genes play a role in MV replication in vivo, we have studied the replication of these mutants in the SCID-hu thy/liv model. In addition, the growth of a virus with a mutation which results in a two- to fivefold increase in levels of V has been characterized. The F 5′UTR and C protein may be accessory elements required for efficient virus growth since peak titers of mutant viruses were lower than those for the parent. Production of virus was delayed and prolonged in the absence of V, while excess V resulted in more rapid viral replication. Data showing that thymocyte and implant survival are prolonged despite the production of large amounts of virus late after infection with the V− mutant suggest V may also play an additional role in pathogenesis of MV infection of thymus.

MATERIALS AND METHODS

Viruses and cells. EdTag, del5F, C−, V−, and V+ strains were constructed and rescued as described previously (38, 39, 43). Vero cells (American Type Culture Collection) were used for growth of virus stocks and plaque assays. Viruses were diluted in Dulbecco modified Eagle medium (DMEM; GIBCO, Grand Island, N.Y.) containing 2% fetal calf serum (FCS; GIBCO) prior to inoculation.

Infection of thy/liv implants. Implants were engrafted under the renal capsule of male homozygous CB-17 *scid*/*scid* mice as described previously (33). For infection, SCID-hu mice were anesthetized with metofane. The left kidney was dissected and externalized. Visible implants were inoculated with 1,000 PFU of virus in 25 μl, using a tuberculin syringe. On the day of harvest, mice were sacrificed and the left kidney with associated implant was removed en bloc. Implants were then divided into thirds for plaque assay, cell counts, and histology. For plaque assay and cell counts, implants were dissected away from the underlying kidney. For histologic analysis, the kidney was not removed.

Virus growth in thy/liv implants. MV growth was assessed by plaque assay. One third of each implant was homogenized in 1 ml of DMEM containing 10% FCS, and serial 10-fold dilutions of this stock were titered. Vero cell monolayers were incubated with the inoculum for 60 min at 37°C, overlaid with 0.6% agar–MEM–1% FCS, and incubated for 5 days at 37°C. Plaques were visualized by staining with 1% crystal violet after fixation with 9% formaldehyde–phosphate-buffered saline (PBS). The statistical significance of plaque assay data was assessed by Student's *t* test, using StatView software (Abacus Concepts, Berkeley, Calif.). Samples showing no growth were assumed to be inoculum failures and were excluded from calculation of the geometric mean titer unless histologic evidence of viral cytopathic effect was present. For statistical analysis, these samples were assigned a value of 1.4 ($\log_{10}$), a value just below the sensitivity of detection of the plaque assay. A single data point (EdTag, day 7 postinfection) which differed from the mean by more than 2 standards of deviation was excluded from analysis.

Thymocyte cell number and flow cytometric analysis. On the day of harvest, one third of each implant was gently disrupted between glass microscope slides into PBS–2% FCS. Organ debris was removed by filtration through 30-μm-pore-size nylon (SpectraMesh, Spectrum, Houston, Tex.). Viable cells were quantitated by staining an aliquot of the cell suspension with 0.05% trypan blue. For flow cytometric analysis, 10^6 cells were stained with fluorescein isothiocyanate (FITC)-labeled anti-CD3 antibody (PharMingen, San Diego, Calif.) for 60 min at 4°C. In the final 15 min of staining, propidium iodide (PI; Molecular Probes, Eugene, Oreg.) was added to stain dead thymocytes. Cells were then washed twice with PBS–2% FCS and analyzed with FACSCaliber instrumentation (Becton Dickinson, Mountain View, Calif.); 10^5 ungated fluorescent events were acquired. Data were analyzed with CellQuest software (Becton Dickinson). The mononuclear cell population displaying variable size and low complexity on forward and side scatter plots was gated for analysis of CD3 and PI staining. Small, low-complexity events representing debris were excluded from analysis.

Thymus histology and immunofluorescence assay. For histologic analysis, one third of each implant was either fixed for 24 to 72 h in 4% paraformaldehyde (PF)–PBS or frozen in Tissue-Tek OCT (Miles, Elkhart, Ind.) on dry ice. After embedding in paraffin, PF-fixed implants were cut into 4-μm sections and stained with hematoxylin and eosin. For detection of MV and cellular antigens, frozen implants were cut into 5- to 7-μm sections. Sections were allowed to dry almost to completion to facilitate adherence to slides and then kept moist in PBS–2% FCS at 4°C to preserve viral and cellular antigens prior to fixation. Sections were fixed in acetone for 5 min at −20°C and allowed to dry briefly. After fixation, slides were kept horizontal to prevent loss of thymocytes in subsequent incubations. Prior to staining, sections were blocked with PBS–2% FCS. MV antigens were detected by indirect staining with a cocktail of monoclonal antibodies against N (N25; WHO Antibody Bank), M (CV-7; gift of Paul Rota), and H (NC32; gift of Bracha Rager-Zisman), each at 1:200 in PBS–2% FCS, followed by biotinylated goat anti-mouse immunoglobulin G (10 μg/ml; Molecular Probes) and streptavidin Texas red (Dupont NEN, Boston, Mass.). Cytokeratin (clone C-11; Sigma, St. Louis, Mo.) and CD15 (clone DU-HL60-3; Sigma) were detected by direct staining using FITC-conjugated primary antibodies. Indirect staining preceded direct staining. All blocking and antibody incubation steps were performed for 60 min at 4°C. Sections were washed three times with ice-cold PBS after each incubation. Coverslips were mounted by using PermaFluor aqueous medium (Immunon, Pittsburgh, Pa.). Immunofluorescence was assessed by epifluorescence microscopy using Nikon Eclipse instrumentation.

Sequence analysis of recovered viruses. Virus stocks for sequence analysis were prepared by passaging homogenates from plaque assays twice on Vero cells. Total cellular RNA was recovered after the second passage with RNAStat (TelTest, Friendswood, Tex.) according to the manufacturer's protocol. MV RNA was amplified by reverse transcription (RT)-PCR. cDNA synthesis reaction mixtures consisted of one half of the recovered RNA, 250 μM deoxynucleoside triphosphates (Boehringer Mannheim, Indianapolis, Ind.), 8 mM dithiothreitol (GIBCO-BRL), 20 U of RNasin (Promega Biotech, Madison, Wis.), 0.8 μg of random hexamer oligonucleotides (Boehringer Mannheim), 1× RT buffer (GIBCO-BRL), and 200 U of SuperScriptII (GIBCO-BRL). Prior to use in RT reactions, RNA was heated to 70°C for 5 min and cooled at room temperature for 5 min. RT reaction mixtures were incubated at 37°C for 60 min. PCR mixtures contained 5 μl of cDNA, 200 μM nucleoside triphosphates (Boehringer Mannheim), 1.25 U of *Taq* polymerase (Boehringer Mannheim), 1× PCR Buffer (Boehringer Mannheim), and 200 nM each primer. Primers used to amplify the region surrounding the editing site within the P cistron were 5′-GCTCCTGAG ACTCCAATC-3′ (forward) and 5′-GGGATCTCGGGGAATTG-3′ (reverse). PCR cycling conditions consisted of 95°C for 1 min, followed by 30 cycles of 95°C for 15 s and 55°C for 30 s. PCR products were finished with 60°C incubation for 6 min. Following PCR, amplified fragment size was assessed by agarose gel electrophoresis. PCR products from reactions that amplified a fragment of expected length were further purified on Qiaquick columns (Qiagen, Santa Clarita, Calif.) according to the manufacturer's protocol. Eluted products were resuspended in distilled water and sequenced with a primer complementary to a sequence internal to the synthesized fragment (5′-CTCCGCCCCCGGACCCC G-3′), using ABI Prism instrumentation (Perkin-Elmer, Foster City, Calif.) at the Johns Hopkins DNA Synthesis Core Facility.

RESULTS

Replication of recombinant MV strains in thy/liv implants. The growth of five recombinant MV strains, the parental virus and four mutant viruses, was assessed in thymic implants (Fig. 1). The recombinant parental virus (EdTag) is an extensively passaged, molecularly cloned, sequenced derivative of the Edmonston B strain of MV. Three nucleic acid substitutions in the noncoding region between N and P genes were introduced to allow the distinction of recombinant virus from the standard Edmonston B strain. Four mutant viruses were constructed in this background to allow assessment of the function of the F 5′UTR and the C and V proteins (Fig. 1). The mutations consisted of a 504-nucleotide deletion of the 5′ noncoding region of the fusion gene (del5F), two nucleotide substitutions altering the initiator methionine codon and creating a new stop codon six amino acids into the C ORF (C−), a single nucleotide substitution which abrogates the recognition of the editing site in the P ORF required for the synthesis of V mRNA (V−), and insertion of three G residues at the P ORF editing site (V+) which increases V expression two- to fivefold in Vero cells (43). Three nucleotides were deleted in the H-L intergenic region of this virus in order to preserve the rule of six.

Implants were inoculated directly with 10^3 PFU of virus and were harvested at various times postinfection. The parental virus EdTag reached peak titer of approximately 10^5 PFU/third of implant between 3 and 7 days postinfection (Fig. 2). Titers declined 100-fold by 28 days postinfection, presumably due to virus-induced death of the susceptible cells. Growth of the mutant viruses in thy/liv implants was distinct from that of EdTag. The peak titers for del5F and C− were 10-fold less than that of EdTag (Fig. 2A and C; C−, $P = 0.02$; del5F, $P = 0.007$), but the kinetics of replication differed only slightly. Virus production 4 days after infection was 10-fold greater in del5F-infected than in EdTag-infected implants, but this difference did not reach statistical significance ($P = 0.08$). EdTag reached a peak at day 7 and declined thereafter, while C− and del5F continued at peak levels of replication through day 14 postinfection and then declined at a rate similar to that for EdTag (Fig. 2A).

Occasionally, virus was not detected by plaque assay after inoculation of implants. Such implants were excluded from calculation of the geometric means (Fig. 2A) and thymocyte viability (Fig. 3) unless there was evidence of viral cytopathic effect. A lack of growth was observed most often in implants infected with the C− mutant (4 of 8 implants [Fig. 2C]) but was also seen in implants inoculated with EdTag (2 of 10 implants) and del5F (1 of 11 implants) 7 days after infection (Fig. 2C). It is unclear whether the lack of growth in a greater number of implants infected with C− was due to technical reasons since the data were obtained from four separate inoculations.

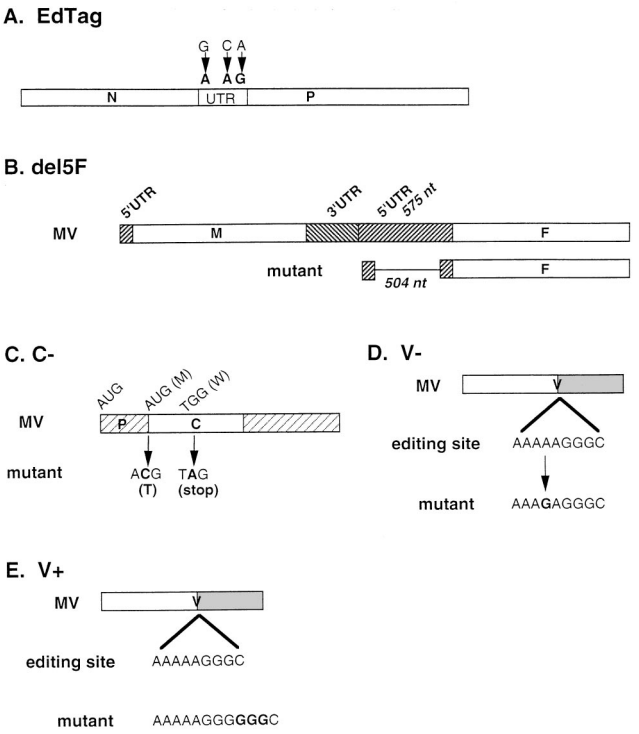

FIG. 1. Recombinant MVs. Nucleotides representing site-specific mutations are shown in boldface. (A) The three nucleotide changes in the noncoding region between N and P in EdTag are indicated. These changes are also present in all mutant constructs. (B) The 504-nucleotide (nt) deletion of the F 5′UTR of del5F is indicated by the thin line. (C) The wild-type initiation methionine and tryptophan codon six amino acids downstream are indicated above the C gene. Mutations are shown below. The first mutation was predicted to inactivate the initiator methionine. The second mutation created a stop codon after the first five amino acids of the C ORF. (D) V-mutant, created by a single A-to-G substitution shown in boldface within the P ORF. □, shared amino terminus of V and P; ▨, unique carboxy terminus of V. (E) V+, insertion of three G residues at the editing site within the P ORF shown in boldface. Boxes and shading as in panel D.

V− and V+ viruses grew with kinetics substantially different from those for EdTag. V− replication was delayed and prolonged. Peak titer was achieved by day 14 for V−, compared to day 7 postinfection for EdTag, and large amounts of virus continued to be produced 28 days after infection (Fig. 2B). At 47 days after infection, V− mutant-infected implants were still producing high levels of virus (mean titer, 4.4 $\log_{10}$ PFU/third of implant). In contrast, V+ grew rapidly, producing 100-fold more virus than EdTag after 4 days of infection ($P = 0.02$ [Fig. 2B]). Viral replication continued at high levels until day 14 postinfection and decreased in parallel with EdTag through 28 days postinfection. Peak titers for V−, V+, and EdTag were not significantly different. All thy/liv-passaged mutant strains demonstrated plaque morphologies comparable to that of EdTag on Vero cells.

Effect of recombinant MV replication on implant thymocytes. Previous study of MV replication in thy/liv implants

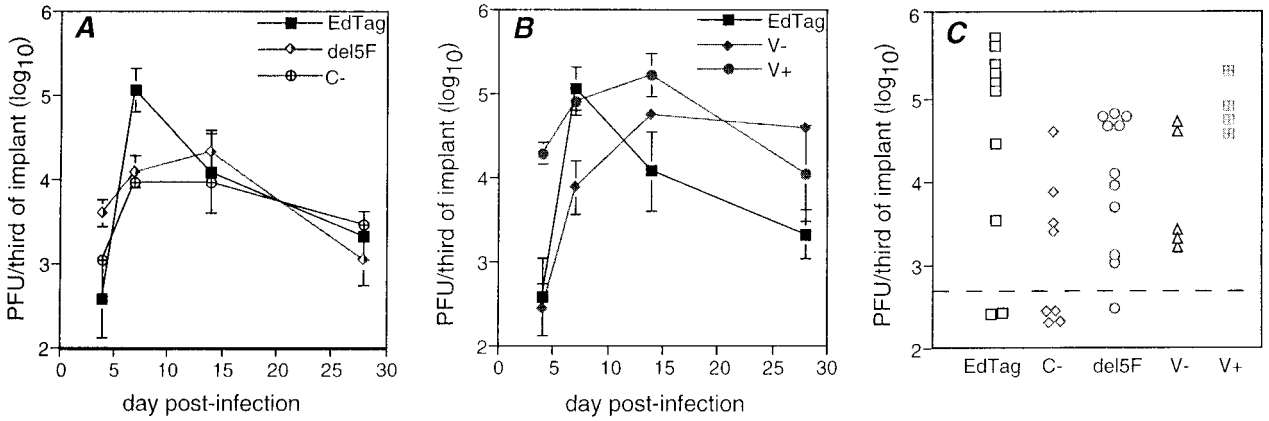

FIG. 2. Growth of recombinant mutant MVs in SCID-hu thy/liv implants. Implants were infected with 10^3 PFU of virus and harvested at various times postinfection. (A) Growth of C− and del5F compared to that of EdTag; (B) growth of V− and V+ compared to that of EdTag. Each point is the geometric mean of 2 to 10 mice. Error bars indicate the standard errors of the means. (C) Scatter plot of the amount of virus in individual implants 7 days after infection. The dotted line represents the lower limit of detection of the plaque assay. Data from four different experiments are shown.

demonstrated that MV infects thymic stromal epithelial cells and cells of the monocyte/macrophage lineage but not thymocytes. However, thymocyte apoptosis and a decline in thymocyte number is induced by infection with virulent strains. To assess the effect of recombinant mutant MV infection on thymocyte viability, thymus cells were collected at various times after infection. Viability was assessed by light microscopy using trypan blue exclusion and by flow cytometry using PI coupled with anti-CD3 for identification of thymocytes. C− and del5F caused a 10-fold decrease in the numbers of viable cells 28 days after infection, which was similar to that caused by EdTag (Fig. 3A). A decrease in mononuclear cells was also seen by flow cytometry. Forward and side scatter plots showed predominantly debris with a reduction of events in the mononuclear cell region (Fig. 4A). Very few $CD3^+$ PI^- cells remained 28 days postinfection (Fig. 4B).

Virus mutants which had opposing effects on growth kinetics also had opposing effects on thymocyte viability within infected implants. After 28 days, viable thymocyte numbers declined 10-fold in implants infected with V+, similar to the effect of EdTag (Fig. 3B). This decrease was confirmed by flow cytometry, which demonstrated a reduction in the number of $CD3^+$ PI^- cells in the mononuclear cell region (Fig. 4). In contrast, although implants infected with the V− mutant continued to produce high levels of virus, numbers of viable thymocytes declined less than fivefold after 28 days of infection. By flow cytometry, a large number of events were still detected in the mononuclear cell gate (Fig. 4A), and the percentage of $CD3^+$ PI^- cells in the total population changed minimally (Fig. 4B).

Effect of MV replication on implant architecture. The histologic morphology of MV-infected thy/liv implants was assessed by hematoxylin-and-eosin staining. In previous studies, implants infected with the low-passage-number MV isolate Chi-1 manifested marked thymocyte pyknosis and nuclear condensation by day 4 and complete loss of thymocytes by day 14 (2). The onset and progression of histopathologic changes was slower in implants infected with EdTag. Thymus morphology was relatively normal through 14 days postinfection (data not shown). However, the effects of viral replication were evident by 28 days postinfection, when implants infected with EdTag, del5F, C−, and V+ demonstrated marked cortical and medullary thymocyte loss and thymic involution (Fig. 5), providing histologic correlation of the effect of these viruses on thymocyte number. In marked contrast, the histology of thymuses infected with the V− mutant strain remained similar to that of

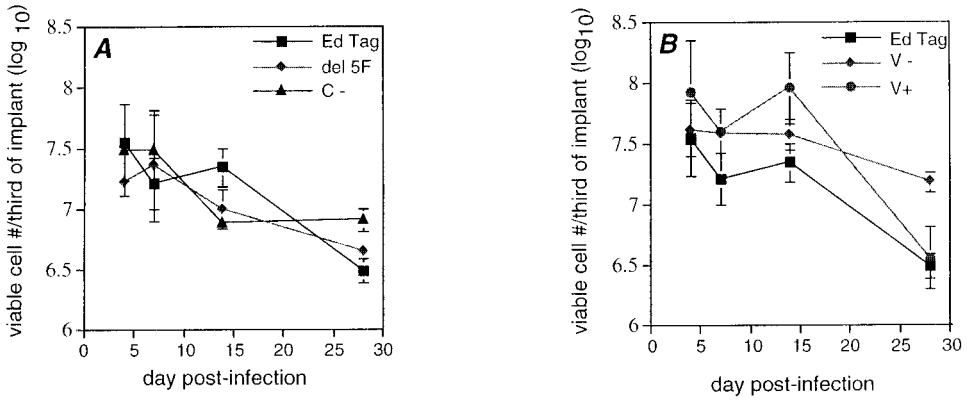

FIG. 3. Effect of recombinant mutant MV infection on numbers of viable thymocytes in SCID-hu thy/liv implants. Thymocytes were released from implants, and viability was assessed by trypan blue exclusion. Points represent the geometric means of data from implants which were used in the calculation of geometric mean titers in Fig. 2. Error bars indicate the standard errors of the means. (A) Effects of infection with del5F, C−, and EdTag on thymocyte survival compared to EdTag; (B) Effect of infection with V−, V+, and EdTag on thymocyte survival.

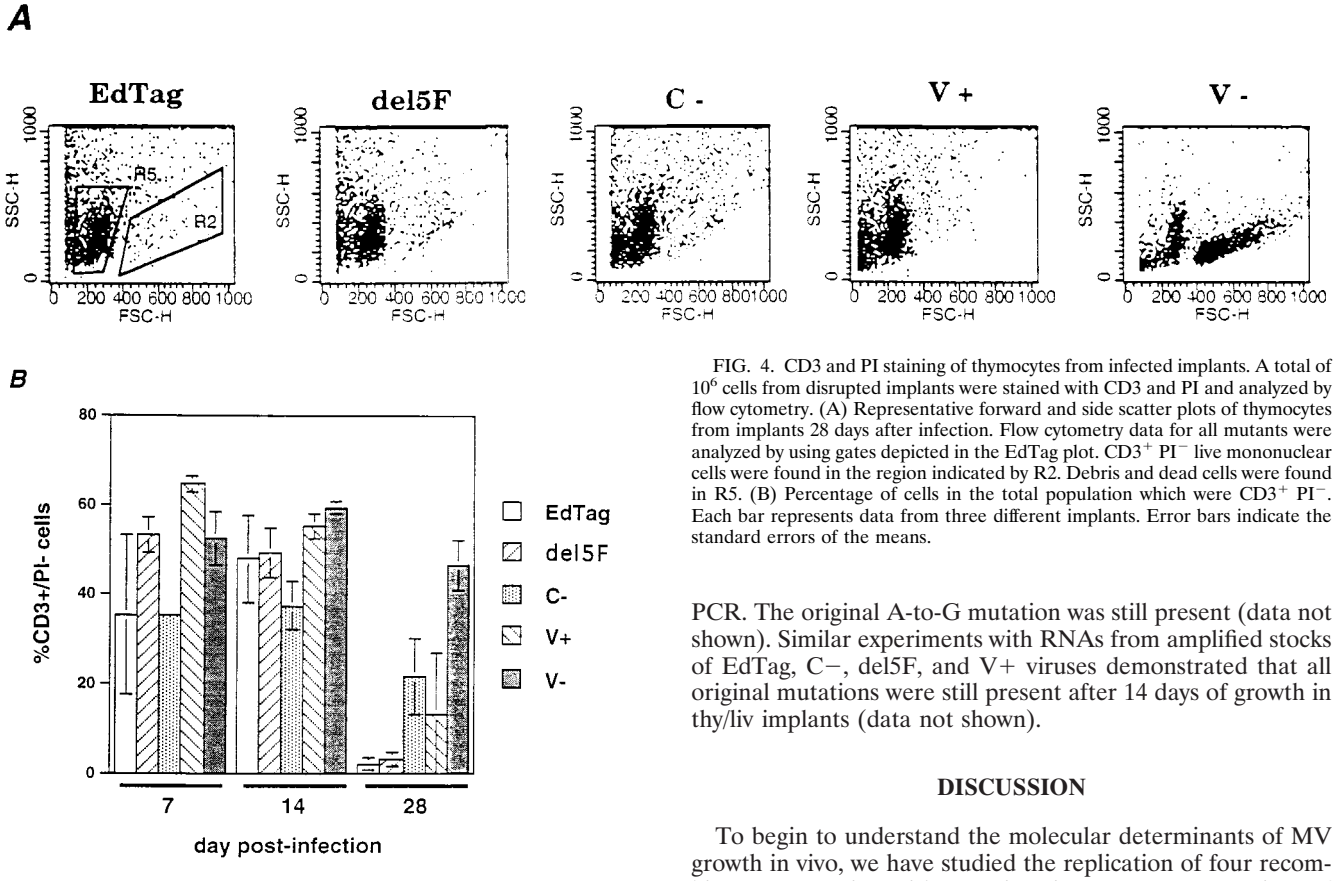

FIG. 4. CD3 and PI staining of thymocytes from infected implants. A total of 10^6 cells from disrupted implants were stained with CD3 and PI and analyzed by flow cytometry. (A) Representative forward and side scatter plots of thymocytes from implants 28 days after infection. Flow cytometry data for all mutants were analyzed by using gates depicted in the EdTag plot. $CD3^+$ PI^- live mononuclear cells were found in the region indicated by R2. Debris and dead cells were found in R5. (B) Percentage of cells in the total population which were $CD3^+$ PI^-. Each bar represents data from three different implants. Error bars indicate the standard errors of the means.

mock-infected implants even after 47 days of infection (Fig. 5F).

Localization of V− replication thy/liv implants. To determine whether V− retained the in vivo cellular tropism of EdTag, the cell types infected by the V− mutant were identified by dual-label immunofluorescence. Infected cell types were identified by costaining with anti-CD15 antibody to identify resident monocytes/macrophages or with anticytokeratin antibody to identify thymic stromal epithelial cells. MV antigens were found in medullary zones and colocalized with cells expressing CD15 (Fig. 6D to F) and cytokeratin (Fig. 6A to C) in V− mutant-infected implants. In addition, MV antigens were found in Hassall's corpuscles adjacent to MV-infected stromal cells (Fig. 6A to C). A similar pattern of colocalization and distribution was demonstrated in implants infected with EdTag (data not shown) and the Chi-1 isolate of MV (2). No immunofluorescence was detected on sections of MV-infected implants stained with secondary antibody and avidin Texas red or on sections of mock-infected implants stained with the cocktail of monoclonal anti-MV antibodies, demonstrating that indirect staining for MV antigens was specific. These results suggest that the altered phenotype of the V− strain cannot be explained by a change in cell tropism.

Sequence of viruses recovered from infected implants. To determine whether a reversion of the editing site mutation occurred in V− mutant-infected implants after 28 days of replication, isolated virus was sequenced. A virus stock was prepared from homogenates used in plaque assays by passage on Vero cells. MV-specific sequences were amplified by RT-PCR. The original A-to-G mutation was still present (data not shown). Similar experiments with RNAs from amplified stocks of EdTag, C−, del5F, and V+ viruses demonstrated that all original mutations were still present after 14 days of growth in thy/liv implants (data not shown).

DISCUSSION

To begin to understand the molecular determinants of MV growth in vivo, we have studied the replication of four recombinant MV strains, with mutations in genes or gene regions of unknown function, in a unique human thymus model which faithfully duplicates in vivo virulence phenotypes of MV (2). The data show that these mutant strains have altered growth characteristics in vivo. Deletion of the F 5′UTR and abrogation of C expression resulted in decreased peak virus production and small changes in the kinetics of growth. The effects of these viruses on implant architecture and thymocyte death were similar to those of the parent EdTag. In contrast, mutations which affected V expression altered the kinetics of virus growth but had no effect on peak virus production. The kinetics of virus growth correlated with the level of V expression. V−, which fails to express V due to an A-to-G substitution in the fourth position in the editing site, grew slowly, and growth was prolonged. Large amounts of virus continued to be produced as late as 47 days postinfection. V+, a mutant which produces elevated levels of V, had the opposite effect on virus growth. High levels of virus were produced early in infection, suggesting that V overexpression conferred an initial growth advantage, but growth declined by 28 days after infection. These two mutant strains also had opposite effects on thymocyte viability and implant architecture. Infection with V+, like parent virus infection, induced a decline in thymocytes and disruption of implant architecture. In contrast, thymocytes were only minimally affected by V− infection and implant architecture remained well preserved.

EdTag, the parent virus in these studies, is a derivative of Edmonston B which has been passaged extensively in tissue culture cells. Despite its passage history, this virus grew well in thy/liv implants. However, it did show some signs of attenuation. Peak virus production was reduced approximately 10-fold

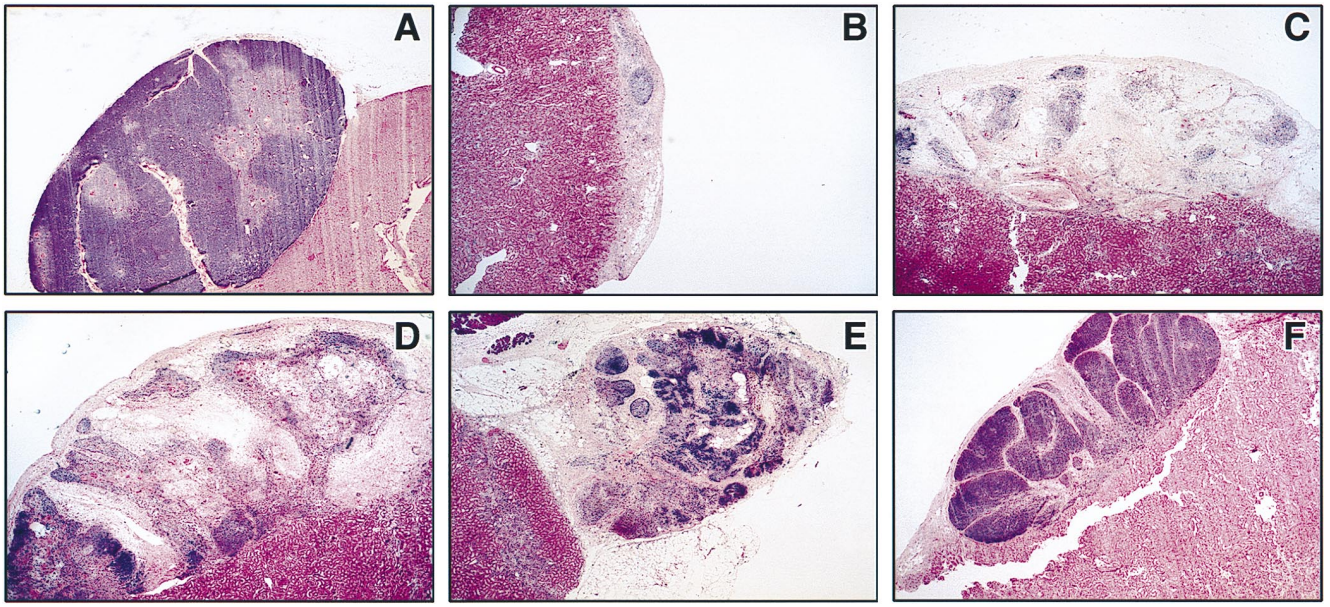

FIG. 5. Histology of implants 28 to 47 days after infection with recombinant mutant MVs. One third of each implant was fixed in 4% PF–PBS. Sections were stained with hematoxylin and eosin. Attached renal tissue lies underneath thymus implants. (A) Mock-infected implant showing intact cortical and medullary zones, day 28; (B) EdTag, day 28; (C) del5F, day 28; (D) C−, day 28; (E) V+, day 28; (F) V−, day 47. Magnifications: A, ×16; B to F, ×20.

compared to Chi-1, a patient isolate which has been passaged minimally. EdTag also grew more slowly than Chi-1, producing peak titers at 7 days rather than 3 days after infection, and viral cytopathic effect occurred later. Finally, thymocyte apoptosis, which correlates with virus virulence (2), was delayed after infection with EdTag. Implants were largely devoid of thymocytes by 14 days postinfection with Chi-1, compared to 28 days after infection with EdTag.

The growth of del5F, C−, and V− in SCID-hu thy/liv implants demonstrates that the F 5′UTR, the C protein, and the V protein are not absolutely required for MV replication in this system. However, they may have accessory functions required for efficient MV replication given the phenotypes of decreased peak virus production and altered growth kinetics seen in viruses with mutations in these genes. Additionally, construction of these mutations in the parental background of a more virulent virus like Chi-1 might result in more dramatic effects on virus growth.

The effect of the F 5′UTR on F expression during MV infection of the thy/liv implant is unknown. The phenotype of

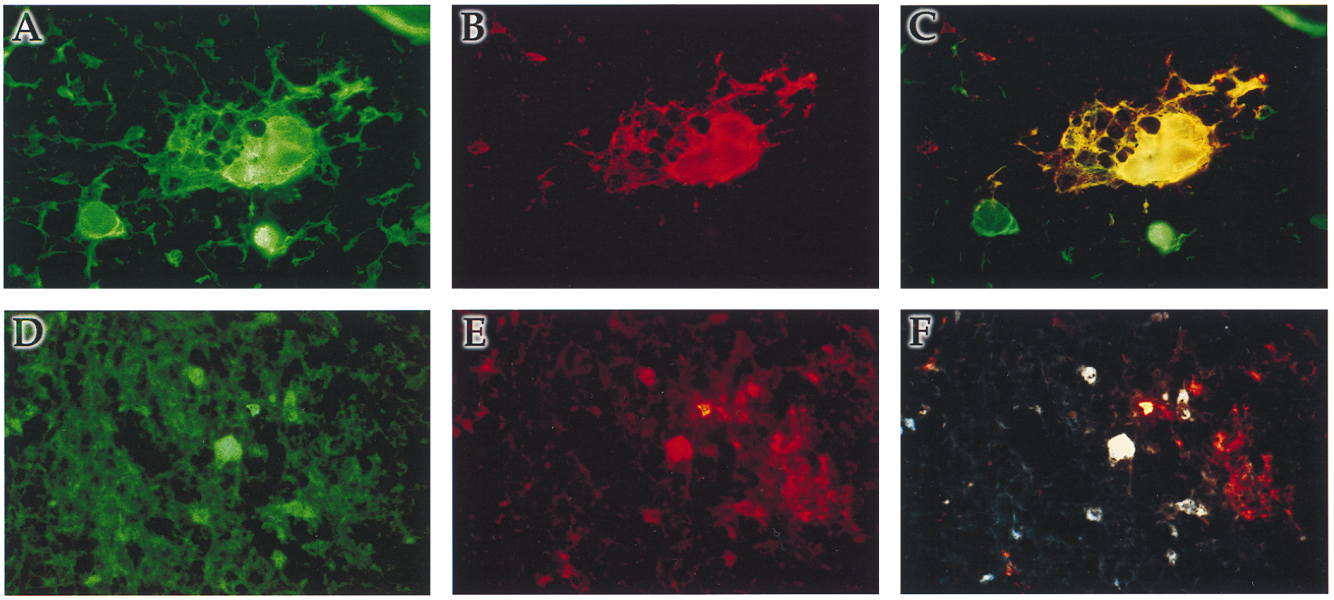

FIG. 6. Immunofluorescence staining of thy/liv implant infected with V−. At day 7 postinfection, one third of an implant was frozen in OCT. Sections were stained for MV antigens by using monoclonal antibodies against H, N, and M followed by biotinylated anti-mouse immunoglobulin G and streptavidin Texas red (B and E). Cell types were labeled with FITC-conjugated anticytokeratin antibody (A) or FITC-conjugated anti-CD15 antibody (D). (C) Colocalization of immunofluorescence in panels A and B. (F) Colocalization of immunofluorescence in panels D and E.

the del5F mutant in thy/liv implants is consistent with a functional alteration leading to a change in the level, but not the abrogation, of F expression. To determine the effect of this deletion in thy/liv implants, it will be important to characterize the level of F mRNA and protein expression. A decrease in F expression would suggest that the F 5′UTR acts as a positive regulator of translation. However, the phenotype of an early growth advantage combined with decreased peak titer observed for the del5F mutant is also consistent with a negative regulatory activity of the F 5′UTR. High levels of F synthesis might lead to increased virus production early in infection and might also cause premature fusion and death of infected cells prior to peak virus production. Additionally, it is possible that the function of the F 5′UTR is partially preserved since approximately 70 nt of this region are present in the del5F mutant. Construction and testing of a mutant bearing a deletion of the remaining sequence will be required to fully assess the function of the 5′UTR.

The phenotypes of V− and V+ suggest that V expression regulates the rate of MV growth in thy/liv implants. V expression also affects the growth of SeV in vivo. However, unlike the delayed and prolonged growth of MV V−, virus production in the lungs of immunocompetent mice infected with SeV V− mutants declines rapidly after an initial rise (23, 24). Viral antigen expression is also reduced and restricted within the respiratory epithelium (23). The in vivo observations for these two viruses are apparently conflicting but may be explained by differences in immune responses. In the lungs of immunocompetent mice, inefficient virus spread may facilitate early activation of a local immune response and lead to accelerated SeV clearance. The SCID mice with thy/liv implants cannot mount antiviral B- and T-cell responses. Thus, inefficient spread may lead to delayed and prolonged growth. How the V protein might control virus spread is unclear. The SeV V protein binds soluble nucleoprotein and inhibits genomic RNA synthesis. Inefficient spread might result from aberrant regulation of genomic RNA synthesis. Alternatively, the V protein may have other novel functions in vivo or different roles in the pathogenesis of MV and SeV infection.

Prolonged viral replication combined with thymocyte and implant survival after infection with the MV V− strain suggests that V may play a role in MV pathogenesis in addition to growth regulation. Dual-immunofluorescence studies suggest that these observations cannot be accounted for by a change in tropism leading to loss of the ability of MV V− to infect stromal epithelial cells. An alternative hypothesis to explain sustained virus production and thymocyte survival is that V plays a role in a process leading to the death of infected cells. In the absence of V, infected stromal epithelial cells and monocytes would survive, virus replication would continue, and thymocytes would remain viable because trophic signals required for survival, such as interleukin-7, would be maintained. Alternatively, V might induce signals which cause thymocyte apoptosis such as Fas ligand, tumor necrosis factor, or local production of glucocorticoids. However, this hypothesis does not account for continued virus production. It is also possible that altered virus growth and thymocyte survival are due to increased P expression rather than decreased V expression since mutation of the editing site would result in the exclusive synthesis of phosphoprotein from the P ORF. In infection with the Edmonston strain of MV, 50% of the mRNA expressed from the P ORF is V mRNA (9).

Since the function of the C protein during MV replication is not well characterized, the mechanism leading to diminished peak virus production in implants infected with C− is unclear. In SeV infection, C may regulate the switch to genomic RNA synthesis by preferentially inhibiting mRNA and antigenome synthesis from the le+ promoter (6, 45) and may facilitate virus growth by preventing replication from suboptimal promoters, such as mRNAs that are mistakenly packaged into nucleocapsids (45). Interestingly, in the lungs of immunocompetent mice, SeV C− growth declines rapidly, suggesting that a defect in replication leads to rapid clearance similar to SeV V− (17).

Whether MV C functions like SeV C during infection of thy/liv implants is unknown. The low peak titer of C− could result from the inefficient switch to genome synthesis or from decreased polymerase selectivity. Alternatively, although SeV and MV are related viruses, their replication mechanisms may not be exactly the same and their C proteins may have shared but not identical functions. For example, C may enforce the rule of six, which is observed by both viruses (7, 39, 45). Other C functions may be quite different, as suggested by the effect of the C protein on the recovery of infectious virus from transfected plasmids. MV can be rescued from transfected plasmids expressing C (39), while SeV can be recovered only if C expression is inhibited (6, 17).

The significance of the inability to detect virus growth in a greater number of implants infected with C− is unclear. It might be explained by technical difficulties or implant conditions at the time of inoculation. However, a variable ability to support MV replication has also been observed in human peripheral blood lymphocytes infected with C− (33a). Since MV C associates with cellular proteins (28), it may regulate virus growth through an interaction with cellular factors whose expression varies from host to host.

Finally, disparities in the determinants for growth in vitro and in vivo have been reported for a growing number of viruses. For example, glycoprotein C is dispensable for growth of herpes simplex virus and varicella-zoster virus in tissue culture (11, 29), but viruses lacking expression of glycoprotein C have reduced infectivity in human skin implants engrafted in SCID mice (32). The accessory protein Nef is dispensable for HIV and simian immunodeficiency virus replication in vitro (1, 21, 25), but mutants bearing *nef* deletions are severely attenuated in SCID-hu thy/liv implants (1, 21) and rhesus macaques (25). Similar results have been demonstrated for the HIV genes *vpu* and *vif* (1). These findings support one of the fundamental hypotheses of viral pathogenesis, that the determinants of virus growth in organs comprised of numerous interacting cell types at various stages of differentiation and with variable capacity to divide are much more complex than those required for replication of virus in a clonal population of dividing cells growing in defined tissue culture medium.

ACKNOWLEDGMENTS

We thank Paul Rota, Bracha Rager-Zisman, and the WHO Antibody Bank for generous gifts of monoclonal antibodies. We also thank Michael Teng, Mari Manchester, and Andy Golden for helpful discussion and suggestions.

This work was supported by research grants from the World Health Organization (D.E.G.), by grants R01AI23047 (D.E.G.), R01AI35136 (M.A.B.), T32AI07417 (A.V.), and T32AI07541 (A.V.) from the National Institutes of Health, and by grant 31-43475.95 from the Schweizerische Nationalfonds (M.A.B.).

REFERENCES

1. **Aldrovandi, G. M., and J. A. Zack.** 1996. Replication and pathogenicity of human immunodeficiency virus type 1 accessory gene mutants in SCID-hu mice. J. Virol. **70:**1505–1511.
2. **Auwaerter, P. G., H. Kaneshima, J. M. McCune, G. Wiegand, and D. E. Griffin.** 1996. Measles virus infection of thymic epithelium in the SCID-hu mouse leads to thymocyte apoptosis. J. Virol. **70:**3734–3740.

3. **Bellini, W. J., G. Englund, S. Rozenblatt, H. Arnheiter, and C. D. Richardson.** 1985. Measles virus P gene codes for two proteins. J. Virol. **53:**908–919.
4. **Bonyhadi, M. L., L. Rabin, S. Salimi, D. A. Brown, J. Kosek, J. M. McCune, and H. Kaneshima.** 1993. HIV induces thymus depletion in vivo. Nature **363:**728–732.
5. **Brown, J. M., H. Kaneshima, and E. Mocarski.** 1995. Dramatic intrastrain differences in the replication of human CMV in SCID-hu mice. J. Infect. Dis. **171:**1599–1603.
6. **Cadd, T., D. Garcin, C. Tapparel, M. Itoh, M. Homma, L. Roux, J. Curran, and D. Kolakofsky.** 1996. The Sendai paramyxovirus accessory C proteins inhibit viral genome amplification in promoter-specific fashion. J. Virol. **70:**5067–5074.
7. **Calain, P., and L. Roux.** 1993. The rule of six, a basic feature for efficient replication of Sendai virus defective interfering RNA. J. Virol. **67:**4822–4830.
8. **Cathomen, T., D. J. Buchholz, P. Spielhofer, and R. Cattaneo.** 1995. Preferential initiation at the second AUG of the measles virus F mRNA: a role for the long untranslated region. Virology **214:**628–632.
9. **Cattaneo, R., K. Kaelin, K. Baczko, and M. A. Billeter.** 1989. Measles virus editing provides an additional cysteine-rich protein. Cell **56:**759–764.
10. **Cattaneo, R., and J. K. Rose.** 1993. Cell fusion by the envelope glycoproteins of persistent measles viruses which caused lethal human brain diseases. J. Virol. **67:**1493–1502.
11. **Cohen, J. I., and K. E. Seidel.** 1994. Absence of varicella-zoster virus (VZV) glycoprotein V does not alter growth of VZV in vitro or sensitivity to heparin. J. Gen. Virol. **75:**3087–3093.
12. **Curran, J., M. DeMelo, S. Moyer, and D. Kolakofsky.** 1991. Characterization of the Sendai virus V protein with an anti-peptide antiserum. Virology **184:**108–116.
13. **Curran, J. A., and D. Kolakofsky.** 1988. Ribosomal initiation from an ACG codon in the Sendai virus P/C mRNA. EMBO J. **7:**245–251.
14. **Delenda, C., S. Hausmann, D. Garcin, and D. Kolakofsky.** 1997. Normal cellular replication of Sendai virus without the trans-frame, nonstructural V protein. Virology **228:**55–62.
15. **Enders, J. F., and T. C. Peebles.** 1954. Propagation in tissue cultures of cytopathic agents from patients with measles. Proc. Soc. Exp. Biol. Med. **86:**277–286.
16. **Evans, S. A., G. J. Belsham, and T. Barrett.** 1990. The role of the 5′ nontranslated regions of the fusion protein mRNAs of canine distemper virus and rinderpest virus. Virology **177:**317–323.
17. **Garcin, D., M. Itoh, and D. Kolakofsky.** 1997. A point mutation in the Sendai virus accessory C protein attenuates virulence for mice, but not virus growth in cell culture. Virology **238:**424–431.
18. **Gupta, K. C., and S. Patwardhan.** 1988. ACG, the initiator codon for a Sendai virus protein. J. Biol. Chem. **263:**8553–8556.
19. **Horikami, S. M., R. E. Hector, S. Smallwood, and S. A. Moyer.** 1997. The Sendai virus C protein binds the L polymerase protein to inhibit viral RNA synthesis. Virology **235:**261–270.
20. **Horikami, S. M., S. Smallwood, and S. A. Moyer.** 1996. The Sendai virus V protein interacts with the NP protein to regulate viral genome RNA replication. Virology **222:**383–390.
21. **Jamieson, B. D., G. M. Aldrovandi, V. Planelles, J. B. M. Jowett, L. Guo, L. Bloch, and J. A. Zack.** 1994. Requirement of human immunodeficiency virus type 1 Nef for in vivo replication and pathogenicity. J. Virol. **68:**3478–3485.
22. **Jamieson, B. D., G. M. Aldrovandi, and J. A. Zack.** 1996. The SCID-hu mouse: an in vivo model for HIV-1 pathogenesis and stem cell gene therapy for AIDS. Semin. Immunol. **8:**215–221.
23. **Kato, A., K. Kiyotani, Y. Sakai, T. Yoshida, and Y. Nagai.** 1997. The paramyxovirus, Sendai virus, V protein encodes a luxury function required for viral pathogenesis. EMBO J. **16:**578–587.
24. **Kato, A., K. Kiyotani, Y. Sakai, T. Yoshida, T. Shioda, and Y. Nagai.** 1997. Importance of the cysteine-rich carboxy-terminal half of V protein for Sendai virus pathogenesis. J. Virol. **71:**7266–7272.
25. **Kestler, H. W., D. J. Ringler, M. Kazuyasu, D. L. Panicali, P. K. Sehgal, M. D. Daniel, and R. C. Desrosiers.** 1991. Importance of the nef gene for maintenance of high virus loads and for development of AIDS. Cell **65:**651–662.
26. **Lin, G. Y., R. G. Paterson, and R. A. Lamb.** 1997. The RNA binding region of the paramyxovirus SV5 V and P proteins. Virology **238:**460–469.
27. **Liston, P., and D. J. Briedis.** 1994. Measles virus V protein binds zinc. Virology **198:**399–404.
28. **Liston, P., C. DiFlumeri, and D. J. Briedis.** 1995. Protein interactions entered into by the measles virus P, V, and C proteins. Virus Res. **38:**241–259.
29. **Manservigi, R., P. Spear, and A. Buchan.** 1977. Cell fusion induced by herpes simplex virus is promoted and supported by different glycoproteins. Proc. Natl. Acad. Sci. USA **74:**3913–3917.
30. **Mocarski, E. S., M. Bonyhadi, J. M. McCune, and H. Kaneshima.** 1993. Human CMV in a SCID-hu mouse: thymic epithelial cells are prominent targets of viral replication. Proc. Natl. Acad. Sci. USA **90:**104–108.
31. **Moffat, J. F., M. D. Stein, H. Kaneshima, and A. M. Arvin.** 1995. Tropism of varicella-zoster virus for human $CD4^+$ and $CD8^+$ T lymphocytes and epidermal cells in SCID-hu mice. J. Virol. **69:**5236–5242.
32. **Moffat, J. F., L. Zerboni, P. R. Kinchington, C. Grose, H. Kaneshima, and A. M. Arvin.** 1998. Attenuation of the vaccine Oka strain of varicella-zoster virus and role of glycoprotein C in alphaherpesvirus virulence demonstrated in the SCID-hu mouse. J. Virol. **72:**965–974.
33. **Namikawa, R., K. N. Weilbaecher, H. Kaneshima, E. J. Lee, and J. M. McCune.** 1989. Long-term human hematopoiesis in the SCID-hu mouse. J. Exp. Med. **172:**1055–1063.

33a. **Naniche, D.** Personal communication.

34. **Numazaki, K., H. Goldman, I. Wong, and M. A. Wainberg.** 1989. Replication of measles virus in cultured human thymic epithelial cells. J. Med. Virol. **27:**52–58.
35. **Paterson, R. G., G. P. Leser, M. A. Shaughnessy, and R. A. Lamb.** 1995. The paramyxovirus SV5 V protein binds two atoms of zinc and is a structural component of virions. Virology **208:**121–131.
36. **Patwardhan, S., and K. C. Gupta.** 1988. Translation initiation potential of the 5′ proximal AUGs of the polycistronic P/C mRNA of Sendai virus: a multipurpose vector of site-specific mutagenesis. J. Biol. Chem. **263:**4907–4913.
37. **Precious, B., D. F. Young, A. Bermingham, R. Fearns, M. Ryan, and R. E. Randall.** 1995. Inducible expression of the P, V, and NP genes of the paramyxovirus simian virus 5 in cell lines and an examination of NP-P and NP-V interactions. J. Virol. **69:**8001–8010.
38. **Radecke, F., and M. A. Billeter.** 1996. The nonstructural C protein is not essential for multiplication of Edmonston B strain measles virus in cultured cells. Virology **217:**418–421.
39. **Radecke, F., P. Spielhofer, H. Schneider, K. Kaelin, M. Huber, C. Dotsch, G. Christiansen, and M. A. Billeter.** 1995. Rescue of measles virus from cloned DNA. EMBO J. **14:**5773–5784.
40. **Randall, R. E., and A. Bermingham.** 1996. NP:P and NP:V interactions of the paramyxovirus simian virus 5 examined using a novel protein:protein capture assay. Virology **224:**121–129.
41. **Richardson, C., D. Hull, P. Greer, K. Hasel, A. Berkovich, G. Englund, W. Bellini, B. Rima, and R. Lazzarini.** 1986. The nucleotide sequence of the mRNA encoding the fusion protein of measles virus (Edmonston strain): a comparison of fusion proteins from several different paramyxoviruses. Virology **155:**508–523.
42. **Sakaguchi, M., Y. Yoshikawa, K. Yamanouchi, T. Sata, K. Nagashima, and K. Takeda.** 1986. Growth of measles virus in epithelial and lymphoid tissues of cynomolgus monkeys. Microbiol. Immunol. **30:**1067–1073.
43. **Schneider, H., K. Kaelin, and M. A. Billeter.** 1997. Recombinant measles virus defective for RNA editing and V protein synthesis are viable in cultured cells. Virology **227:**314–322.
44. **Takeuchi, K., K. Tanabayashi, M. Hishiyama, Y. Yamada, A. Yamada, and A. Sugiura.** 1990. Detection and characterization of mumps virus V protein. Virology **178:**247–253.
45. **Tapparel, C., S. Hausmann, T. Pelet, J. Curran, D. Kolakofsky, and L. Roux.** 1997. Inhibition of Sendai virus genome replication due to promoter-increased selectivity: a possible role for the accessory C protein. J. Virol. **71:**9588–9599.
46. **Thomas, S. M., R. A. Lamb, and R. G. Paterson.** 1988. Two mRNAs that differ by two nontemplated nucleotides encode the amino coterminal proteins P and V of the paramyxovirus SV5. Cell **54:**891–902.
47. **Valsamakis, A., F. Mustafa, D. E. Griffin, and H. L. Robinson.** Unpublished data.
48. **Vidal, S., J. Curran, and D. Kolakofsky.** 1990. Editing of the Sendai virus P/C mRNA by G insertion occurs during mRNA synthesis via a virus-encoded activity. J. Virol. **64:**239–246.
49. **Wardrop, E. A., and D. J. Briedis.** 1991. Characterization of V protein in measles virus-infected cells. J. Virol. **65:**3421–3428.
50. **White, R. G., and J. F. Boyd.** 1986. The effect of measles on the thymus and other lymphoid tissues. Clin. Exp. Immunol. **30:**1067–1073.
51. **Yamada, H., T. Omata-Yamada, J. Taira, K. Mizumoto, and K. Iwasaki.** 1990. Association of the Sendai virus C protein with nucleocapsids. Arch. Virol. **113:**245–253.